PHILOSOPHICAL TRANSACTIONS OF THE ROYAL SOCIETY A MATHEMATICAL, PHYSICAL & ENGINEERING SCIENCES

The Nonlinear Dynamics of Journal Bearings

J. Brindley, M. D. Savage and C. M. Taylor

Phil. Trans. R. Soc. Lond. A 1990 **332**, 107-119
doi: 10.1098/rsta.1990.0103

The nonlinear dynamics of journal bearings

By J. Brindley,[1] M. D. Savage[1] and C. M. Taylor[2]

Departments of Applied Mathematical Studies[1] and Mechanical Engineering[2] and Centre for Nonlinear Studies, University of Leeds, Leeds LS2 9JT, U.K.

The journal bearing is ubiquitous in moving mechanical systems, and is a major potential target for study in the field of lubrication theory. Despite this, theoretical understanding of its dynamic behaviour is far from complete; in particular the essentially nonlinear interplay of rotor dynamics and fluid dynamics of the lubricant has been studied only very recently. Our own investigations have been mainly numerical, and have revealed a wide range of qualitative behaviour. They have confirmed the great importance of cavitation of the lubricant, and the sensitivity to geometrical features of the bearing. Additionally they have enabled us to identify the crucial non-dimensional parameters and their critical values. Finally they have stimulated analytical approaches (e.g. searches for Hopf bifurcations).

In this paper we exploit the conceptual approach of dynamical systems theory to present many of our results in a succinct form. Our aim is to make clear not only the extent of understanding of the problem, but also the present shortcomings of theory that require further study.

1. Introduction

The journal or rotor bearing is familiar to all engineers; indeed it is virtually ubiquitous in moving mechanical systems. The basic configuration consists of a journal or rotor, of cylindrical shape, turning relative to a surrounding bearing (or stator). Each component is usually circular, or nearly so; efficient operation requires the presence of a fluid lubricant in the space between them. Physical contact between the journal and the bearing usually results in a failure of the system (in practice often spectacularly so), and a satisfactory operating state must not permit this to occur. This requirement clearly puts a tight geometrical constraint on the excursions of the centre of the rotor relative to that of the bearing; it must either remain stationary or move in a closed orbit of limited extent. (In a theoretical sense, suitably bounded chaotic motions might not be disastrous; in practice they would almost certainly be undesirable.)

Theoretical models of the system describe the motion of the rotor centre on the basis of newtonian mechanics; the simplest models assume that the rotor and bearing are rigid. The forces acting are, on the one hand, the mass of the rotor together with the load (varying) exerted by the rest of the connected mechanical system, and, on the other hand, the stress exerted by the fluid lubricant on the surface of the rotor. Because the flow of the lubricant is itself driven by the rotor, this is a situation of strong feedback, highly nonlinear for even the crudest models of the fluid flow.

Successful analysis depends on a number of approximations and simplifications, and most of our results (and, as far as we know, all those of other authors) have used

Phil. Trans. R. Soc. Lond. A (1990), **332**, 107–119 *Printed in Great Britain*

the Reynolds approximation to the Navier–Stokes equations of motion for the fluid. Under certain circumstances, however, inertial effects in the lubricant can be important (Collins *et al.* 1986).

Early integrations of the equations of motion were almost entirely numerical, using the Reynolds approximation (Brindley *et al.* 1979). It rapidly became clear that failure of the bearing was inevitable when the lubricating film completely filled the gap between rotor and bearing. Stronger asymmetries of the fluid stress forces than can be produced in such a model are necessary to bound the motion of the rotor centre sufficiently. This result is borne out by practical experience; many 'successful' bearings have geometrical asymmetries, often developed by trial and error. For simplicity we restrict our consideration in this paper to circular shapes for both rotor and bearing; some effects of asymmetric geometry have been reported elsewhere (Brindley *et al.* 1986*a*, *b*).

One flow feature of dominant influence in the case of a liquid lubricant is cavitation of the liquid, usually arising through 'ventilation', the invasion by air of regions of the flow with subambient pressures (Brindley *et al.* 1983). The extent, position and motion of any cavity is of crucial importance in determining the motion of the rotor, and the correct modelling of cavitation is a challenging and important problem. Several reviews exist in the literature (Dowson & Taylor 1979), and we remark on the more widely used models in §2.

We stress in this paper the status of the problem as one of conceptual simplicity but substantial engineering importance and potentially great richness of behaviour. A combination of numerical integrations and analytical methods has revealed the essentials of this behaviour for the unforced, balanced-mass rotor, and established the foundations for the more demanding but realistic situation in which one or more of time varying forcing of the load, mass imbalance, or acceleration of the system as a whole is taken into account.

After establishing in §2 the equations of the mathematical model, we report the results of numerical integrations in §3 and in §4 indicate the way in which analytical techniques, largely motivated and stimulated by the numerical results, have revealed a more full qualitative picture of journal behaviour within the limits of the model. Finally, in §5 we discuss the extent to which general concepts of dynamical systems theory are useful in recognising crucial areas for future investigation.

2. Mathematical models

The configuration of the journal bearing is illustrated in figure 1, in which the main physical dimensions and coordinate systems are indicated. We limit our attention to purely two-dimensional motion of the rotor, and we assume that its rotation rate about its centre A remains at the constant value ω (i.e. we neglect any feedback on the rotation of the rotor about its centre A as a result of the effect of tangential viscous stresses, assuming that the rotor is driven at a constant speed at all times). Thus the dynamics of the rotor are totally represented by the motion of A, and the equations of motion take the form

$$\ddot{\epsilon} - \epsilon\dot{\phi}^2 = \bar{\omega}^{-2}\{\cos\phi + (SF_r/W)\}, \tag{2.1a}$$

$$\epsilon\ddot{\phi} + 2\dot{\epsilon}\dot{\phi} = -\bar{\omega}^{-2}\{\sin\phi - (SF_\phi/W)\}, \tag{2.1b}$$

where ϵ is the eccentricity ratio e/c, ϕ is the attitude angle, F_r, F_φ, are the components

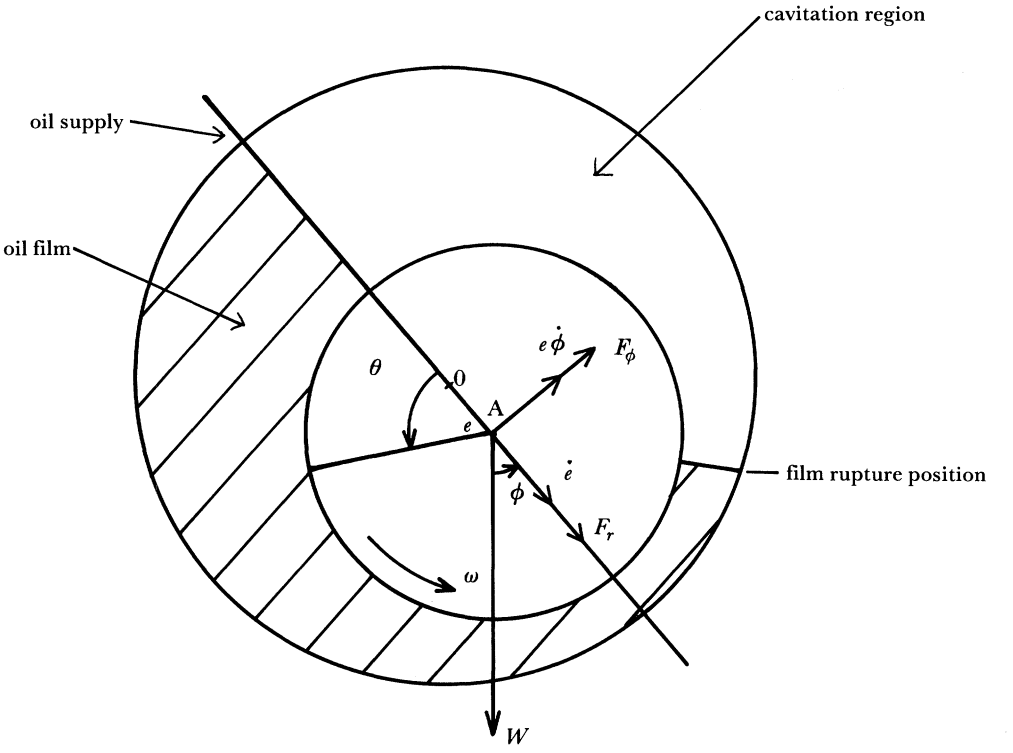

Figure 1. Bearing configuration: bearing centre at 0, rotor centre at A, where 0A = e; radius of rotor is R, of bearing is $R+c$; rotational speed ω; load W; hydrodynamic force components F_r, F_ϕ.

of the total fluid stress in the r and φ directions, and a dot denotes differentiation with respect to the non-dimensional time $\tau = \omega t$. Additionally we have introduced the non-dimensional parameters

$$S = LR^3\mu\omega/Wc^2 \quad \text{(the Sommerfeld number)} \tag{2.2}$$

and

$$\bar{\omega} = \omega\{mc/w\}^{\frac{1}{2}} \quad \text{(a non-dimensional rotation speed).} \tag{2.3}$$

The expressions giving F_r, F_φ are obtained by integrating the pressure forces around the rotor, thus

$$F_r = \int p\cos\theta\,\mathrm{d}s, \quad F_\phi = \int p\sin\theta\,\mathrm{d}s. \tag{2.4}$$

A value of p is obtained from the Reynolds equation

$$\frac{\partial}{\partial\theta}\left\{(1+\epsilon\cos\theta)^3\frac{\partial\bar{p}}{\partial\theta}\right\}+\left(\frac{R}{L}\right)^2\frac{\partial}{\partial z}\left\{(1+\epsilon\cos\theta)^3\frac{\partial\bar{p}}{\partial z}\right\} = 6S\{-\epsilon(1-2\dot{\phi})\sin\theta+2\dot{\epsilon}\cos\theta\}, \tag{2.5}$$

with appropriate boundary conditions for the non-dimensional pressure

$$p = p/\mu\omega(R/c)^2.$$

The choice of these boundary conditions constitutes a major difficulty for the modeller. In practice any cavity which forms is far from two-dimensional and, even in steady-state situations, usually consists of a number of discrete elongated bubbles,

separated by narrow continuous streams of lubricant. In unsteady conditions, as when the rotor centre describes some closed orbit, the appropriate boundary conditions are even less clear and more research is needed.

Our aim in this paper, to expose the journal bearing as an interesting and important problem in nonlinear dynamics, is equally well served by any reasonable choice of cavitation boundary condition (though the actual solutions will of course be much affected), and we refer the reader elsewhere for further details (Dowson & Taylor 1979). The simplest realistic assumption is the so called 'oscillating π-film' condition, in which the cavity always occupies the region $\pi < \theta < 2\pi$, corresponding to

$$p = 0 \quad \text{at} \quad \theta = 0, \quad \text{and} \quad \pi < \theta < 2\pi. \tag{2.6}$$

The outcome of this model, assuming a long-bearing approximation, i.e. neglecting the second term on the left-hand side of equation (2.4), is a pair of expressions for F_r, F_φ of the form

$$F_r = S\{12\pi\epsilon^2(1-2\dot{\phi})+6[\pi^2(2+\epsilon^2)-16](1-\epsilon^2)^{-\frac{1}{2}}\dot{\epsilon}\}/\pi(2+\epsilon^2)(1-\epsilon^2), \tag{2.7}$$

$$F_\phi = S\{6\pi\epsilon(1-\epsilon^2)^{\frac{1}{2}}(1-2\dot{\phi})+24\epsilon\dot{\epsilon}\}/(2+\epsilon^2)(1-\epsilon^2), \tag{2.8}$$

from which the strong nonlinearities of equations (2.1) follow. In engineering practice, many journal bearings have asymmetries associated with slight departures from exactly circular shape, typically in the form of steps or bulges in boundaries, or with the presence of a lubricant inlet in the bearing. These asymmetries have an influence on the flow patterns and pressure conditions, and hence on cavity occurrence and extent. Though their direct effect is small, through these secondary effects they may exert great influence on rotor stability, and mathematical models have been used to explore this effect directly (Brindley *et al.* 1986*b*). The equations of motion for bearing and fluid remain as (2.1) and (2.4), but the conditions on p now become

$$p = 0 \quad \text{at} \quad \pi = \varphi_i, \quad \text{the position of the lubricant inlet,} \tag{2.9}$$

together with

$$p(2\pi+\theta_s) = p(\theta_s)-\Delta p, \quad \text{if} \quad p(\theta_s) > 0 \quad \text{after applying (2.9),} \tag{2.10}$$

or

$$p(2\pi+\theta_s) = p(\theta_s) = 0, \quad \text{if} \quad p(\theta_s) < 0 \quad \text{after applying (2.9),} \tag{2.11}$$

where θ_s is the position of a 'step' on the rotor.

Additionally, we set $p(\theta) = 0$ at all points for which a negative value is predicted when carrying out the calculation of net forces on the rotor. The position of φ_i, which 'locks' one end of the cavity, turns out to be crucial for stability; the position θ_s or (φ_s) of a step is less so, becoming important only when it significantly alters a cavity size.

Fluid inertia effects with no cavitation

In this case the mathematical model can be expressed locally in the form of the two-dimensional unsteady boundary-layer equations (Collins *et al.* 1986)

$$\left.\begin{aligned} p\left(\frac{\partial u}{\partial t}+u\frac{\partial u}{\partial x}+v\frac{\partial u}{\partial y}\right) &= -\frac{\partial p}{\partial x}+\mu\frac{\partial^2 u}{\partial y^2}, \\ 0 &= -\partial p/\partial y, \\ \partial u/\partial x+\partial v/\partial y &= 0, \end{aligned}\right\} \tag{2.12}$$

where

$$x = (R+c)\,\theta, \quad y = R+c-r, \tag{2.13}$$

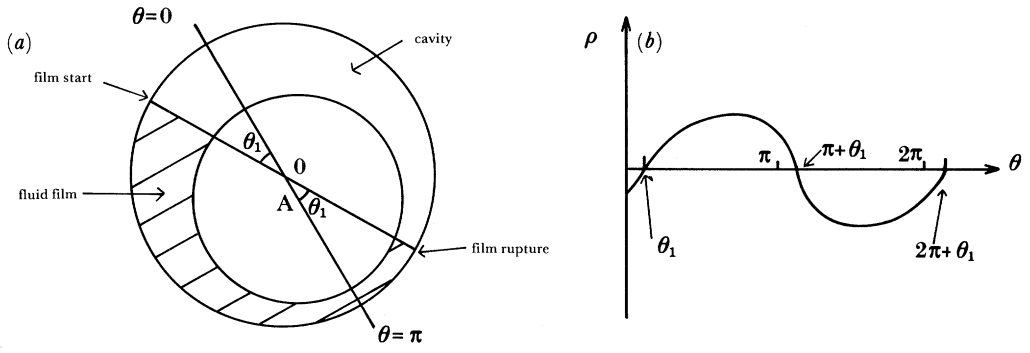

Figure 2. (*a*) Configuration for short bearing as described in text. (*b*) Pressure distribution, $p(\theta)$. In calculating the hydrodynamic force, p is set to zero in the range of θ for which a negative value is obtained from equation (2.4).

subject to the boundary conditions

$$u = v = 0 \quad \text{on} \quad y = 0,$$
$$u = R\omega, \quad v = R\omega\,\partial h/\partial x + \partial h/\partial t \quad \text{on} \quad y \equiv h(x,t) = c[(1+\epsilon\cos\theta)+O(c/R)], \tag{2.14}$$

expressing the full no-slip conditions at the rigid surfaces.

Additionally, since no cavitation is now assumed, we have

$$p(0) = p(2\pi). \tag{2.15}$$

Again, expressions for F_r, F_φ are readily calculated but are rather complicated (Collins *et al.* 1986).

3. Numerical integrations: a glimpse of the picture

The formidable complexities of equations (2.1) with any of the forms for F_r, F_φ arising from particular cavitation assumptions discourage an analytic approach, and, as is the theme of this volume, progress was led by computational effort. Numerical solutions of equation (2.1) for a full film (no cavitation) lubricant invariably indicated failure of the bearing; whatever parameter values and starting conditions where used, the resulting trajectory of the rotor led to collision with the stator (Brindley *et al.* 1979). Cavitation sometimes permitted the existence of stable equilibria or stable closed orbits (limit cycles) and the upshot of many computations was a wide range of apparent behaviour. In addition to stable static states and obvious catastrophic instabilities, small and large stable limit cycles were obtained, and the existence of unstable limit cycles forming boundaries of basins of attraction was surmised (Brindley *et al.* 1979, 1983, 1986*a*, *b*).

We have examined a range of models, assuming several alternative boundary conditions at the cavity–lubricant interface. Results for the short bearing, operating with a cavity occupying the region $\pi+\theta_1 < \theta < 2\pi+\theta_1$, may be used to exemplify the outcome (figure 2).

Here θ_1 is obtained by setting $p = 0$ at θ_1 in the integrated form of equation (2.4) when the term in $\mathrm{d}/\mathrm{d}\theta$ is neglected (short bearing approximation). In fact we find, setting $p = 0$ at $z = 0, L$,

$$\frac{c^2 p}{\mu L^2} = \frac{3z(z-L)}{L^2}\left[\frac{-\epsilon(\omega-2\dot{\phi})\sin\theta+2\dot{\epsilon}\cos\theta}{(1+\epsilon\cos\theta)^2}\right], \tag{3.1}$$

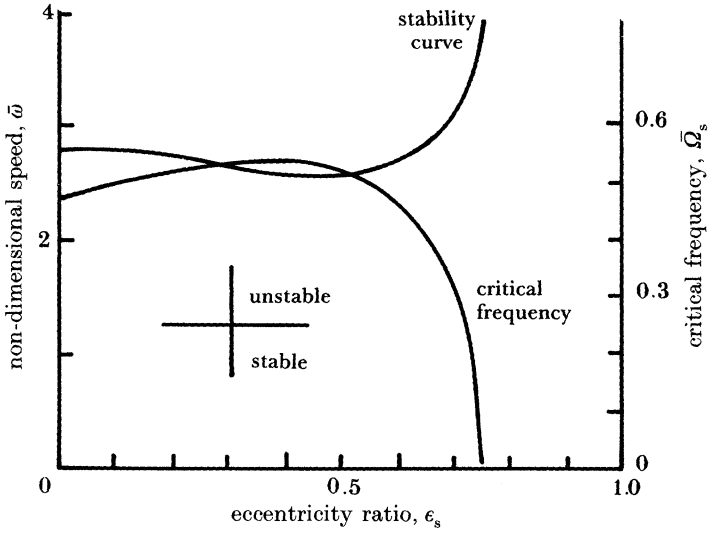

Figure 3. Neutral stability curve as obtained by linear stability theory (upper curve, left-hand scale) and critical frequency as described in §4 (lower curve, right-hand scale).

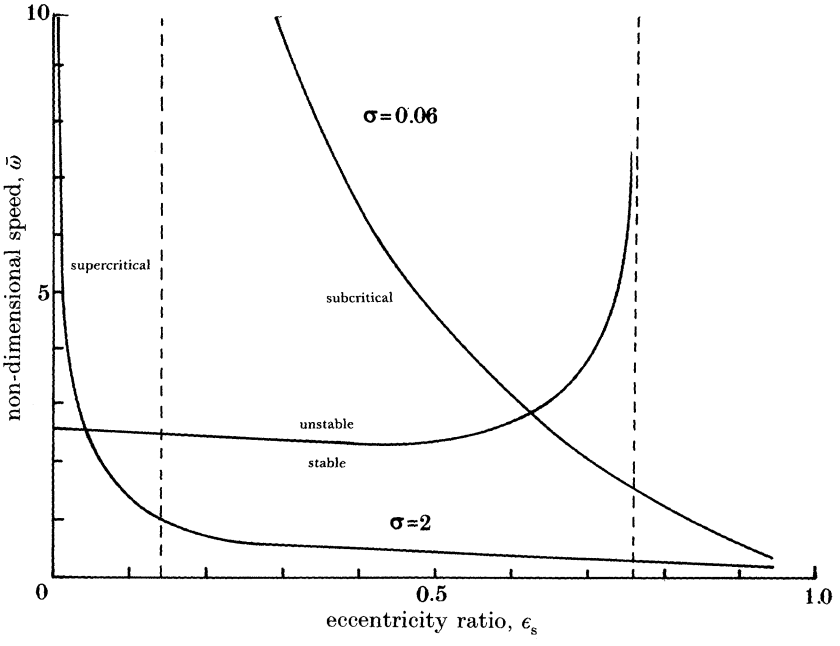

Figure 4. Neutral stability curve and operating curves for $\sigma = 0.06$ and $\sigma = 2.0$. Supercritical and subcritical Hopf bifurcations occur in the regions indicated.

which implies that

$$\tan\theta_1 = 2\dot{\epsilon}/\epsilon(\omega - 2\dot{\phi}). \tag{3.2}$$

Note that, unlike the cruder half-film model for the long bearing, in which the cavity occupies the region $\pi < \theta < 2\pi$, this model permits the cavity to move in response to the dynamical behaviour of the rotor. The actual expressions for F_r, F_φ are very cumbersome and we do not reproduce them here.

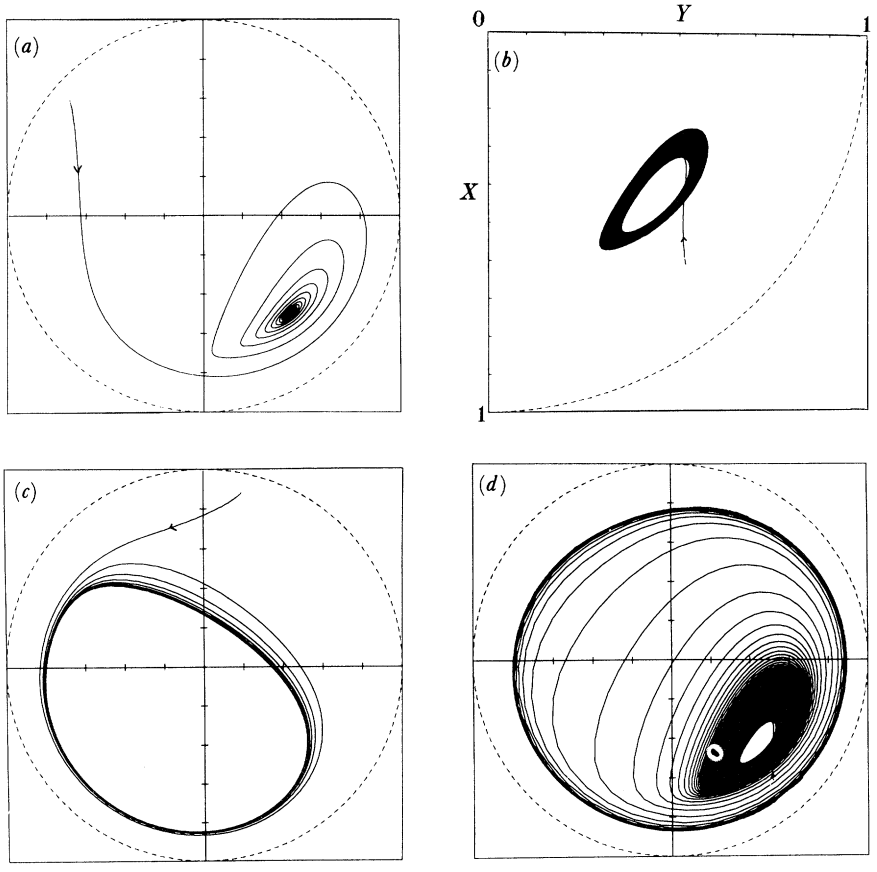

Figure 5. Orbits in the case $\sigma = 0.06$. (*a*) $\bar{\omega} = 2.2$, $\epsilon_0 = 0.9$, $\phi_0 = 4.0$; (*b*) $\bar{\omega} = 2.92$, $\epsilon_0 = 0.8$, $\phi_0 = 0.7$; (*c*) $\bar{\omega} = 2.92$, $\epsilon_0 = 0.8$, $\phi_0 = 0$; (*d*) $\bar{\omega} = 2.96$, $\epsilon_0 = 0.8$, $\phi_0 = 0.7$.

The consequence of a linear analysis of the stability of the equilibrium point (ϵ_s, φ_s) is illustrated in figure 3. The abscissa, ϵ_s, is, of course, not a directly controllable parameter; changes in a real system usually occur through changes in $\bar{\omega}$, and, if all other effects remain constant, it is convenient to define a 'system parameter', $\sigma \equiv L^3 R\mu/(Fmc^5)^{\frac{1}{2}}$, which remains constant throughout the motion.

As $\bar{\omega}$ increases we follow an 'operating curve' in the $(\epsilon_s, \bar{\omega})$ plan as indicated in figure 4 for two values $\sigma = 0.06$, 2.0 respectively.

Traversing the curve $\sigma = 0.06$, we find that, for points well below the neutral stability curve, all orbits are attracted towards the unique steady state (ϵ_s, ϕ_s) (figure 5*a*). When $\bar{\omega}$ is near to $\bar{\omega}_s$ the behaviour depends on initial conditions (ϵ_0, ϕ_0). For a starting position near (ϵ_s, φ_s), we find that orbits are attracted towards the equilibrium point for $\bar{\omega} < \bar{\omega}_s$, and towards a small-amplitude limit cycle for $\bar{\omega} > \bar{\omega}_s$ (figure 5*b*); for a starting position 'far' from (ϵ_s, φ_s) we find an attracting large amplitude limit cycle (figure 5*c*). When $\bar{\omega}$ is considerably larger than $\bar{\omega}_s$, the small amplitude limit cycle disappears (though orbits stay close to it for a long time) and all trajectories are attracted towards the large amplitude limit cycle (figure 5*d*). Eventually as $\bar{\omega}$ increases further this cycle 'hits' $\epsilon = 1$ and the bearing fails.

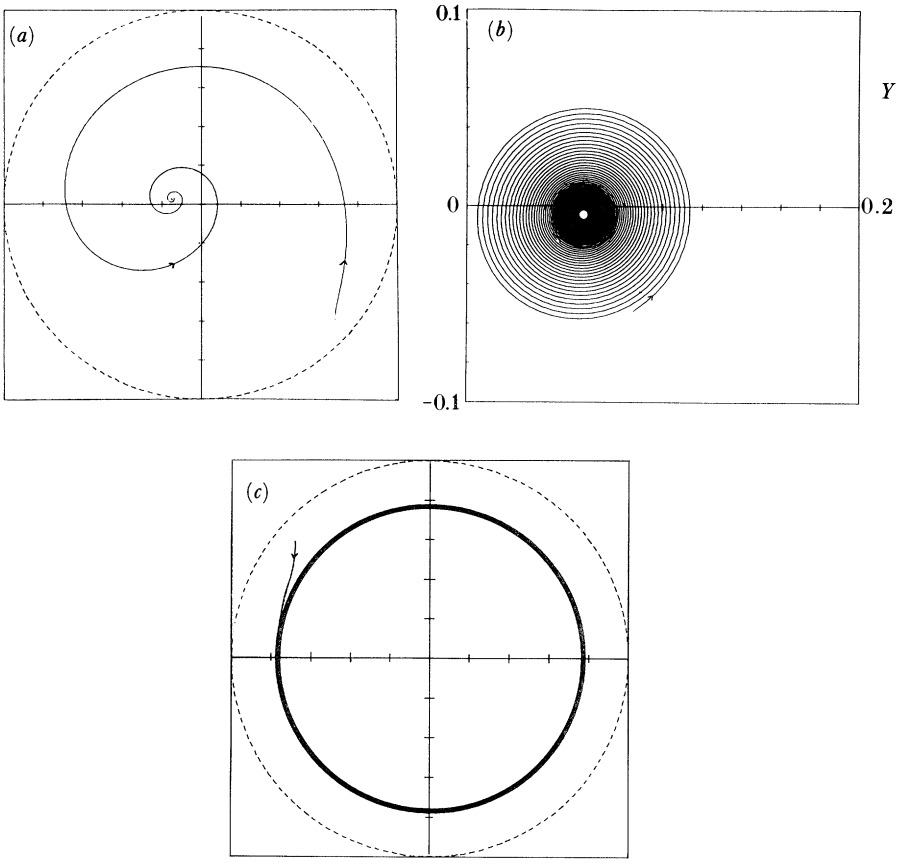

Figure 6. Orbits in case $\sigma = 2.0$. (*a*) $\bar{\omega} = 1.0$, $\epsilon_0 = 0.9$, $\phi_0 = 4.0$; (*b*) $\bar{\omega} = 2.65$, $\epsilon_0 = 0.1$, $\phi_0 = 1.0$; (*c*) $\bar{\omega} = 2.65$, $\epsilon_0 = 0.9$, $\phi_0 = 4.0$.

When $\sigma = 2.0$ we find, for small $\bar{\omega}$, a universally stable equilibrium (ϵ_s, φ_s) as shown in figure 6*a*. For larger $\bar{\omega} < \bar{\omega}_s$ we find a coexisting stable large limit cycle, with final state strongly dependent on initial conditions (figure 6*b*, *c*), and for $\bar{\omega} > \bar{\omega}_s$ we find just the stable large limit cycle, which, as in the earlier case, finally 'hits' the $\epsilon = 1$ barrier. The bifurcational behaviour is summarized in figure 7.

4. Analytical methods

The numerical results, of which those in §3 resemble the tip of a rather large iceberg, reveal a very rich and complex pattern of behaviour, even in this simplest case of an unforced, perfectly balanced, rotor. By their indication of multiple attractors, subcritical as well as supercritical bifurcations, and sensitive dependence on parameter and initial values, they act to stimulate and motivate analytical approaches which might illuminate the global behaviour more fully.

Two lines have been followed; firstly a rigorous approach using the general ideas of bifurcation theory, which is mathematically sound but, in an engineering sense, limited in its range of applicability; secondly an approach in which approximate methods, plausible but on the whole non-rigorous, promise results with a much wider

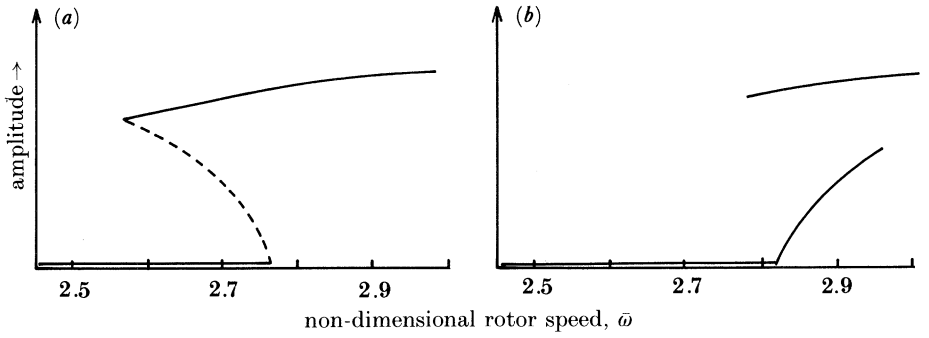

Figure 7. Schematic summary of system behaviour close to the threshold speed for the cases (*a*) $\sigma = 2$ and (*b*) $\sigma = 0.06$. ——, stable; – – –, unstable.

range of use for application. All rigorous approaches are pivoted about the equilibrium state (or states), i.e. solutions of equation (2.1) in which all time derivatives are set to zero. An elementary linear stability analysis quickly reveals neutral stability surfaces in parameter space; a projection of such a surface appears in figure 3. The form of the characteristic equation guarantees that stability is lost when a complex conjugate pair of eigenvalues crosses the imaginary axis with non-vanishing imaginary part, Ω_s, say.

The value of the 'whirl' frequency is also plotted in figure 3, where we have introduced the non-dimensional

$$\bar{\Omega} = \Omega/\omega \tag{4.1}$$

for most of the range of ϵ_s the value of $\bar{\Omega}$ is near to 0.5, falling rapidly to zero as $\epsilon_s \to 0.75$.

The conditions for Hopf bifurcation are met in general, and application of the theory (Gardner *et al.* 1985) reveals that the neutral stability curve may be divided into regions of supercritical bifurcation or subcritical bifurcation, at which stable or unstable limit cycles are shed respectively from the equilibrium point (ϵ_s, φ_s). These results are confirmed and extended to predict the development of small amplitude limit cycles by a multiple scales approach. Numerical continuation methods (Brindley *et al.* 1989) may also be used to extend the bifurcation picture. Good agreement with numerical results is found. Analytical methods for predicting and describing the large amplitude orbits shown in numerical computations are less well advanced and have a much less secure theoretical basis. For this reason they merit a rather more substantial description and justification. A complete exposition will appear elsewhere (Savage *et al.* 1990).

In essence we have used an extension of the harmonic balance method to incorporate higher harmonics and slowly varying amplitudes and phases; we have tentatively called it 'harmonic balance with two timescales'. The approach may be demonstrated by considering a dynamical system of the form

$$\ddot{x} + \omega^2 x = g(x, \dot{x}, t), \tag{4.2}$$

where g is sufficiently smooth and T-periodic in t. It is usual for perturbation techniques to be applied to systems of the form

$$\ddot{x} + \omega^2 x = \epsilon f(x, \dot{x}, t), \tag{4.3}$$

where f is T-periodic and ϵ is an explicit small parameter. Here we rewrite equation (4.2) as

$$\ddot{x}+\omega^2 x=\bar{\mu}f(x,\dot{x},t), \tag{4.4}$$

where $\bar{\mu}$ is an implicit small parameter. Next we assume the solution is dominated by the first harmonic, of frequency ω, with slowly varying amplitude R and phase φ, namely

$$x(t)=R(\tau)\cos(\omega s+\phi(\tau)), \tag{4.5}$$

where s and τ are fast and slow times respectively. In general there will also be a mean (constant or time varying) of the same order as the first harmonic.

Higher harmonics or subharmonics may be readily included, the latter by, for example, taking a form

$$x(t)=Z(\tau)+\sum_{k=0}^{mn}A_k(\tau)\cos\left\{\left(\frac{k\omega s}{n}\right)+\phi_k(\tau)\right\}, \tag{4.6}$$

to truncate the expansion at the mth harmonic.

We now associate the parameter, μ, with the slow timescale, writing

$$s=t, \quad \text{and} \quad \tau=\mu t, \tag{4.7}$$

so that equation (4.2) becomes

$$x''+\omega^2 x=-2\mu\,\partial x'/\partial\tau+\mu f(x,x'+\mu\,\partial x/\partial\tau,s)+O(\mu^2), \tag{4.8}$$

where the dash indicates differentiation with respect to s. Finally, on expanding the right-hand side of equation (4.2) as a Fourier series, we find,

$$x''+\omega^2 x=\mu\sum_{k=0}^{\infty}\{a_k(\tau)\cos n\omega s+b_k(\tau)\sin n\omega s\}. \tag{4.9}$$

The complementary function of (4.9) gives rise to a first harmonic solution, whilst the right-hand side generates higher harmonics of $O(\mu)$ as particular integrals. Hence we see that the assumption that μ is small is the mathematical statement of the fact that the fundamental mode dominates the solution. This implicit small parameter means that we can use the method for arbitrary values of other quantities, such as the amplitude of the orbit or the value of $\omega-\omega_s$, provided that the orbit is well approximated by a single mode.

The removal of secular terms arising from the presence of $\cos\omega_s$ and $\sin\omega_s$ terms on the right-hand side of (4.9) then gives evolution equations for $A(\tau)$ and $\varphi_k(\tau)$ in the usual way. These equations yield results not only for amplitude, but also for stability, and their usefulness with great economy of effort is demonstrated in figure 8, where results for a single term of equation (4.6), i.e. $m=n=0$, are compared with the results obtained by numerical path following techniques in the case of a long bearing approximation with oscillating π-film.

5. Discussion and future development

The journal bearing models we have described comprise a fourth-order nonlinear system of ordinary differential equations (in which the fluid forces are of course consequences of the approximate solution of partial differential equations). We have restricted attention to autonomous equations, and numerical results have prompted the analytical exposure of some of the phenomena characteristic of such a system,

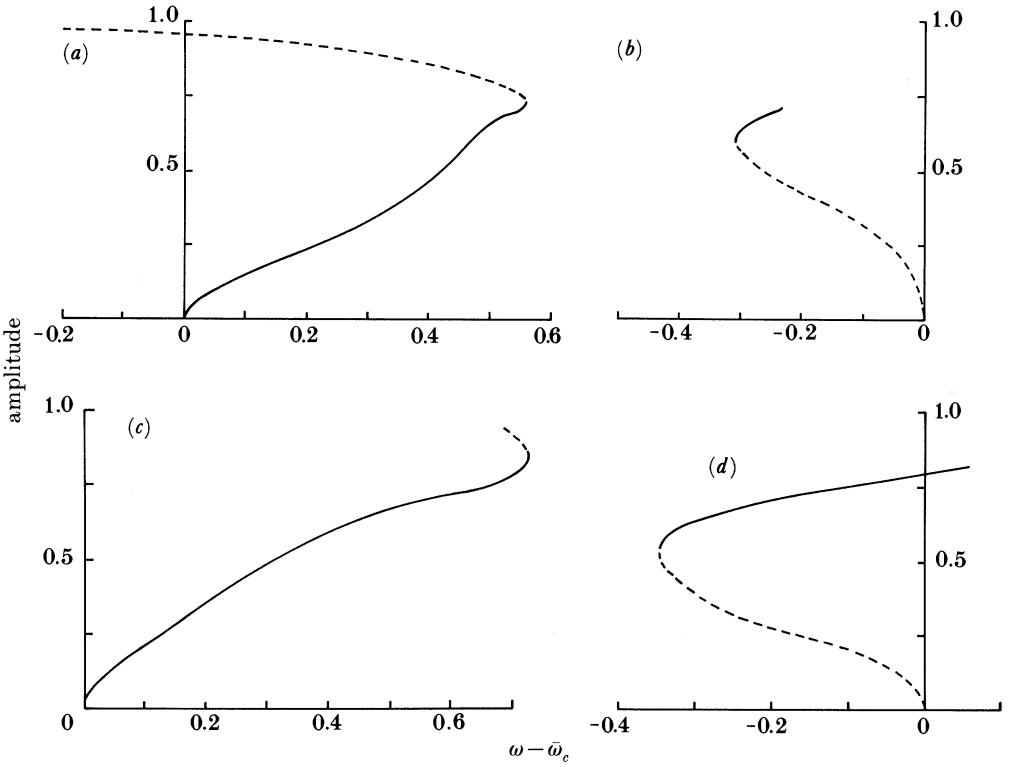

Figure 8. Bifurcation diagrams for $\epsilon_{sc} = 0.6$ and $\epsilon_{sc} = 0.76$ obtained (*a*), (*b*) by using a single term of equation (4.6), and (*c*), (*d*) by full numerical solution of the problem. ——, stable solution; – – –, unstable solution. For (*a*) and (*c*) $\omega_c = 1.37$, for (*b*) and (*d*) $\omega_c = 2.57$.

particularly multiple equilibria, both static and dynamic. Subcritical bifurcations to unstable limit cycles have been identified commonly, and the outlines of a parameter space map of behaviour is clear. Parallel investigations on differing mathematical models arising mainly from alternative cavitation conditions, or the effect of shaft flexibility, have been carried out or are in hand. Though there are very large difference in the position and extent in parameter space of regions with a particular qualitative behaviour, the broad picture is similar (e.g. figure 9) in all cases we have studied.

Interestingly, a quite different nonlinearity, arising from inertia forces in the fluid, is important at relatively low values of ω, and acts to stabilize the equilibrium state in certain circumstances (Collins *et al.* 1986).

For the practising engineer much of value has already emerged, and potential danger areas in parameter space have been pointed. The real challenge, however, still exists, in the form of realistic modelling of the time-dependence of the physical influences. Not only is the load normally a strongly time-varying quantity, quite independently of the motion of the rotor, but dynamic imbalance of the rotor and the use of proper dynamic boundary conditions on the pressure in the lubricant (with subsequent effects on the cavity behaviour) both introduce forcing at the *a priori* unknown frequency of description of any closed orbit. Dynamic imbalance of the rotor of course implies forcing at the imposed speed, ω, of rotation; analysis of this

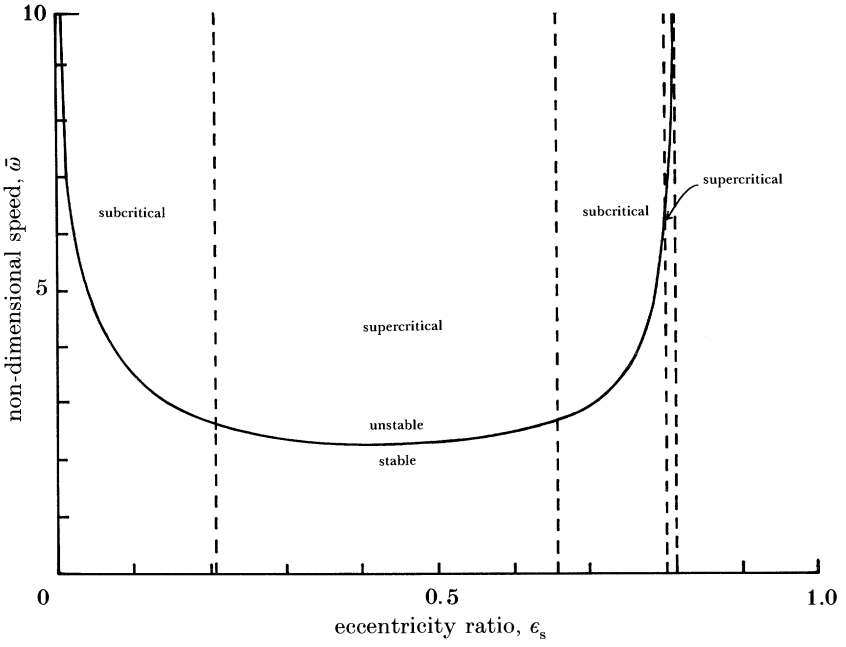

Figure 9. Neutral stability curve for long bearing approximation using the Reynolds boundary condition (oscillatory film, boundary conditions $p = 0$ at $\theta = 0$ and $p = \mathrm{d}p/\mathrm{d}\theta = 0$ at $\theta = \theta_2$, where θ_2 is found by solving $p(\theta_2) = 0$). Regions of supercritical and subcritical Hopf bifurcation indicated.

situation, revealing the expected resonance horns, and a very complex bifurcation picture, has recently been carried out for the long bearing oscillating half film model (Shaw 1989). Much more remains to be done.

The research reported in this paper has benefited from contributions by a number of colleagues, particularly David Collins, Mark Gardner, John McKay and Chris Myers, all sometime research students with us, supported by grants from SERC.

References

Brindley, J., Elliott, L. & McKay, J. T. 1979 Flow in a whirling rotor bearing. *ASME J. appl. Mech.* **46**, 767.

Brindley, J., Elliott, L. & McKay, J. T. 1983 The role of cavitation in whirl instability in a rotor bearing, I and II. *ASME J. appl. Mech.* **50**, 72, 78.

Brindley, J., Elliott, L. & McKay, J. T. 1986*a* Whirl instabilities in pressure-step bearings. *ASME J. appl. Mech.* **53**, 430.

Brindley, J., Elliott, L. & McKay, J. T. 1986*b* The effects of bearing geometry on rotor stability. *ASLE Trans.* **29**, 160.

Brindley, J., Kaas-Petersen, C. & Spence, A. 1989 Path-following methods in bifurcation problems. *Physica* D **34**, 456.

Collins, D., Savage, M. D. & Taylor, C. M. 1986 The influence of fluid inertia on the stability of a plain journal bearing incorporating a complete oil film. *J. Fluid Mech.* **168**, 415.

Dowson, D. & Taylor, C. M. 1979 Cavitation in bearings. *A. Rev. Fluid Mech.* **11**, 35.

Gardner, M., Myers, C. & Savage, M. D. 1985 Analysis of limit-cycle response in fluid film journal bearings. *Q. Jl Mech. appl. Math.* **38**, 27.

Savage, M. D. 1977 Cavitation in lubrication, I. On boundary conditions at fluid–cavity interfaces. *J. Fluid Mech.* **80**, 743.

Savage, M. D., Summers, J. & Brindley, J. 1990 Harmonic balance with two timescales. (In preparation.)

Shaw, J. 1989 Ph.D. thesis, Michigan State University, U.S.A.

PHILOSOPHICAL TRANSACTIONS OF THE ROYAL SOCIETY A MATHEMATICAL, PHYSICAL & ENGINEERING SCIENCES